

Electronic transport properties of nitrogen doped amorphous carbon films deposited by the filtered cathodic vacuum arc technique

This article has been downloaded from IOPscience. Please scroll down to see the full text article.

1998 J. Phys.: Condens. Matter 10 9293

(<http://iopscience.iop.org/0953-8984/10/41/011>)

View [the table of contents for this issue](#), or go to the [journal homepage](#) for more

Download details:

IP Address: 171.66.16.210

The article was downloaded on 14/05/2010 at 17:34

Please note that [terms and conditions apply](#).

Electronic transport properties of nitrogen doped amorphous carbon films deposited by the filtered cathodic vacuum arc technique

X Shi, H Fu, J R Shi, L K Cheah, B K Tay and P Hui

School of Electrical and Electronic Engineering, Nanyang Technological University, Nanyang Avenue, Singapore 2263, Republic of Singapore

Received 16 December 1997, in final form 26 May 1998

Abstract. Highly tetrahedral amorphous carbon thin films were deposited by the filtered cathodic vacuum arc technique at room temperature. Nitrogen was found to be a good n-type dopant of the tetrahedral amorphous carbon thin films. The Fermi level shifts from 0.91 eV above the valence band to 0.65 eV below the conduction band with increasing nitrogen flow rate from null to 16 sccm (nitrogen partial pressure from 0 to 2.4×10^{-4} Torr). At the same time, the optical band gap drops from 2.7 to 1.8 eV. Three electronic transport mechanisms, namely, transport in extended states, in band tails by hopping and variable range hopping (VRH) near the Fermi level, were observed from the thermal activation measurements in the temperature range from 100 to 450 K. The VRH transport parameters for ta-C films are studied, and the density of states near the Fermi level extracted from the hopping transport parameters was found in the range of 6.5×10^{17} – 9.7×10^{19} cm⁻³ eV⁻¹. The dominant doping configuration is the substitution in the sp³ coordination at low N concentration and adoption of sp² bonding at high N concentration.

1. Introduction

Tetrahedral amorphous carbon (ta-C) is an important alternative material for the rare and expensive crystal diamond in a wide range of industrial applications. The electronic properties of amorphous carbon thin films attract more and more attention because of its wide band gap, smooth morphology, high breakdown fields and chemical inertness, which could be suited as material for devices operated at high temperature, high voltage and high radiation environment [1–3]. The filtered cathodic vacuum arc (FCVA) technique has been proven to be promising method to deposit high quality ta-C thin films at room temperature [4]. It was shown by electron energy loss spectroscopy (EELS) [4–6] that as much as 87% of the carbon atoms in the ta-C films form an amorphous tetrahedral (sp³) structure. In the amorphous carbon atom network, the sp³ site forms σ bonds to four adjacent carbon atoms and the sp² site forms three interlayer σ bonds and one weaker π bond. The electronic structure of the amorphous carbons depends primarily on the π states due to their lower energy distances to the Fermi level [7].

Nitrogen doping in the ta-C films is achieved by introducing the nitrogen gas into the arc region of the graphite cathode. The N doping concentration can be controlled by changing the nitrogen gas flow rate (nitrogen partial pressure). In this paper, we concentrate on the nitrogen doping effect on the electronic transport properties. The optical band gap, activation energy, Fermi level shift and hopping characteristic temperature are studied as a function

of the doping nitrogen flow rate. From the hopping transport model at low temperature, information on the density of states $N(E_F)$ near the Fermi level is extracted. The results are discussed in terms of the doping mechanics for ta-C films proposed by Robertson and Davis [8].

2. Experiment details

The FCVA film deposition system has been adequately discussed elsewhere [4]. Carbon ions are produced in a vacuum arc discharge between the cathode and the grounded anode. The cathode is a 60 mm diameter, 99.999% pure graphite target mounted onto a water-cooled stainless-steel block. The arc is ignited by a striker and is afterwards self-sustaining for a few minutes. The arc current is set to 60 A. The macro-particles and neutrals emitted as the cathode erosion by-products are filtered out by using a curvilinear axial magnetic field on a curved toroidal duct. The magnetic field used in the filter region is fixed at 40 mT. A radial electric field is introduced in our system via the torus duct wall bias which substantially increases the plasma throughput [9]. All depositions are carried out at room temperature and the substrate is negatively biased at 80 V, corresponding to 100 eV of impinging carbon ion energy which gives rise maximum sp^3 content [10].

Nitrogen doping is achieved by introducing the nitrogen gas into the cathode arc region. This is different from the method that previous researchers used in their experiments where the gas is either directly fed into the chamber or into the torus [11, 12]. The nitrogen gas is dissociated and ionized by the energetic ions and electrons of the plasma stream. Evidence of the N^+ ions in the plasma was verified by Veerasamy using optical spectroscopy analysis [13]. The chamber background pressure was 2×10^{-6} Torr, and the nitrogen partial pressure varied from 4×10^{-5} Torr to 2.4×10^{-4} Torr when nitrogen flow rate was changed from 2 sccm to 16 sccm. A linear relationship between the nitrogen partial pressure and nitrogen flow rate was found in all experiments. The substrates were (100) n-type silicon and Vitresosil quartz. Activation energy studies were conducted on a gap-cell structure on quartz as well as a sandwich structure on silicon substrate. For the gap-cell structure, a titanium layer was evaporated onto the ta-C thin films as the contact electrodes with a 200 μm wide channel by using the photo-mask. The Ti/ta-C/Ti sandwich structure samples, which were mainly used to measure the very high resistance of some films, were fabricated by depositing titanium and carbon films on n-type (100) Si wafers successively and evaporating another titanium contact with 2 mm in diameter through a shadow mask. The ohmic nature of the contacts was confirmed from the I - V characteristics by using a HP4156 precision semiconductor parameter analyser.

The composition of the N doped ta-C film was determined by using the Rutherford back-scattering (RBS) analysis. The N content was found in the range of 2 at.% to 12 at.% with the nitrogen flow rate changing from 2 to 16 sccm. The thickness of the film was measured by using a Tencor P10 surface profilometer. The optical band gap was determined by Jobin Yvon UVISEL phase modulated spectral ellipsometer. The resistances were measured by using a Keithley 617 electrometer over the temperature range of 100–450 K. A heater stage and a Cryogenic temperature control system were used to obtain a stable temperature.

3. Experimental results

The optical band gap is obtained from the T_{auc} plot, a method common for amorphous materials. A full description of film structure model and simulation parameters used to

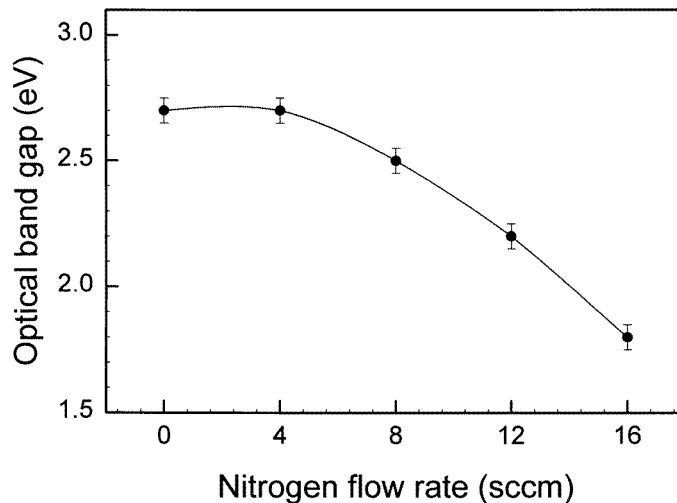


Figure 1. The dependence of the optical band gap on nitrogen flow rate.

determine the optical band gap was reported elsewhere [14]. The optical band gap plotted as a function of the nitrogen flow rate is shown in figure 1. The optical band gap remains constant at 2.7 eV for nitrogen flow rate up to 4 sccm and then decreases from 2.7 to 1.8 eV with an increasing nitrogen flow rate from 4 to 16 sccm.

The conductivity of the thin films was measured at temperature range of 100–450 K by using the gap-cell structure as well as the sandwich structure. Figure 2 shows a typical Arrhenius plot of the conductivity in the whole temperature range. It can be clearly seen that the $\log \sigma$ decreases linearly as $1000/T$ increases with two different slopes in the temperature range above 300 K. At the temperature below 300 K, $\log \sigma$ versus $1000/T$ deviates from a straight line. The temperature dependence of the conductivity for as-deposited and N-doped ta-C films above room temperature is shown in figure 3. A break point was found around the temperature of 380 K which is a similar magnitude to the a-C:H measured by Silva *et al* [15] but larger than the results of Veerasamy *et al* [16]. Since the Arrhenius plot of the conductivity presents a linear relationship over a wide temperature range above 380 K, it can be interpreted that electrical conduction in the high temperature range is induced by the thermal activation of carriers into the extended states and the thermal activation energy can be achieved from the slope. At temperature below 380 K, the Arrhenius plot of each sample changes to another linear relationship, which is characterized by lower activation energies of about 0.1–0.2 eV. This is attributed to the thermally activated carriers into the band tail and the conduction by hopping. The conductivity curves were decomposed into a sum of two exponential functions with the pre-exponential constants of σ_0 (9.2×10^3 – 2.5×10^4 $\text{ohm}^{-1} \text{cm}^{-1}$) and σ_{0hop} (15–80 $\text{ohm}^{-1} \text{cm}^{-1}$) for the extended state conduction and band tail conduction, respectively. This large difference in the pre-exponential constants is consistent with the Mott model [17] that mobility drops drastically at the energy that demarcates the extended states of the valence band or conduction band.

The activation energy extracted from the Arrhenius plot is shown in figure 4 as a function of the doping nitrogen flow rate. The activation energy for the undoped ta-C films is 0.91 eV. It was proved by Frauenheim *et al* [18] through molecular dynamic simulations

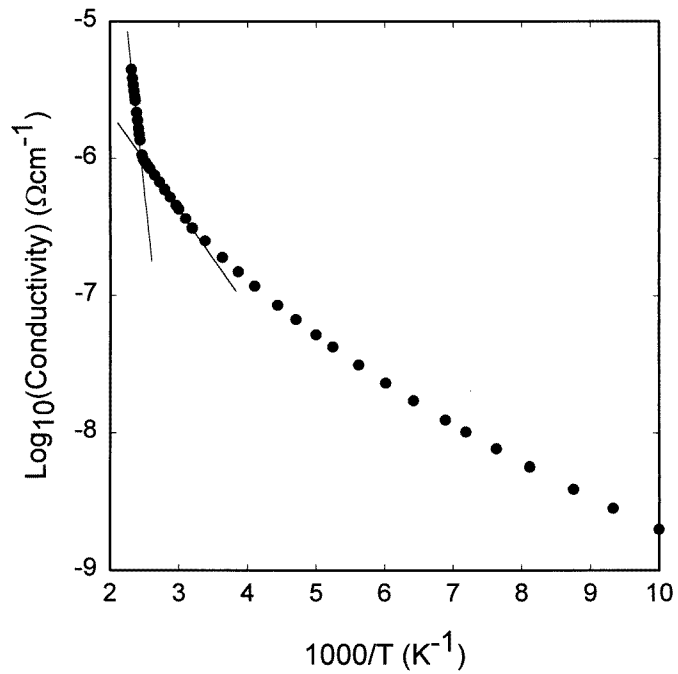


Figure 2. A typical Arrhenius plot of the conductivity of nitrogen-doped ta-C film in the temperature range of 100–450 K. The nitrogen gas flow rate is 12 sccm.

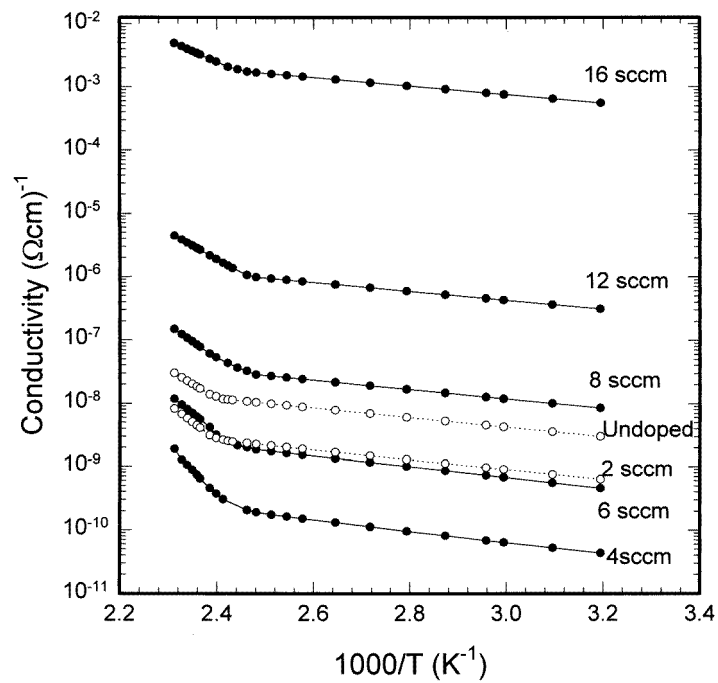


Figure 3. Arrhenius plots of the conductivity of undoped and N-doped ta-C films with different nitrogen flow rates at the temperature between 300 and 450 K.

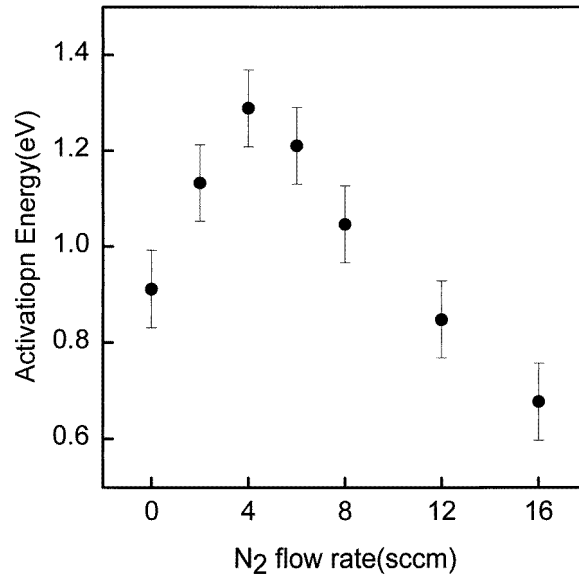


Figure 4. The plot of the activation energy versus nitrogen flow rate.

that the undoped ta-C film is intrinsically p-type because of the structural defects within the amorphous network. The p-type behaviour of the undoped ta-C films was also verified by Amaratunga *et al* [19]. Since the optical band gap of the undoped ta-C film is 2.7 eV (figure 1), its Fermi level is located at 0.91 eV above the valence band and 0.44 eV below the centre of the band gap on the assumption that the mobility gap is taken as equal to the optical Tauc gap. In figure 4, the activation energy shows an initial increase from 0.91 up to 1.29 eV at a nitrogen flow rate of 4 sccm, then decreases gradually to 0.65 eV. This behaviour indicates that there is a gradual shift of the Fermi level towards the middle of the band gap with increasing nitrogen flow rate up to 4 sccm. The ta-C films doped with nitrogen with a flow rate less than 4 sccm can be treated as p-type. When the nitrogen flow rate is larger than 4 sccm, the Fermi level shifts over the midgap. The film is converted from p-type to n-type. The activation energy drops from 1.29 eV at 4 sccm to 0.65 eV at 16 sccm.

The Fermi level position calculated from the optical band gap and activation energy by using the midgap as the reference energy level is shown in figure 5. One can see a clear shift of the Fermi level from 0.44 eV below the midgap for undoped films to 0.22 eV above the midgap at the nitrogen flow rate of 16 sccm. The Fermi level reaches the highest point—0.25 eV above the midgap—at the nitrogen rate of 12 sccm. The slight decrease of the Fermi level at 16 sccm nitrogen rate with respect to that at 12 sccm is caused by the obvious narrowing of the band gap (see figure 1). In diamond, the substituting nitrogen donor occupies a single fixed deep energy level which is located at about 1.4 eV below the conduction band (σ^* states) [8, 20]. For ta-C film, N is a shallow dopant. When the N donor donates an electron to the C defect state near the Fermi level, a positively charged fourfold-coordinated N_4^+ site and a fully filled C state are formed. This behaviour leads to a minor shift of the Fermi level toward the energy level of the N donor site and has a slight doping effect. So the Fermi level shift can be considered as the result of autocompensation between the N donor and the defect states near the Fermi level in the band gap.

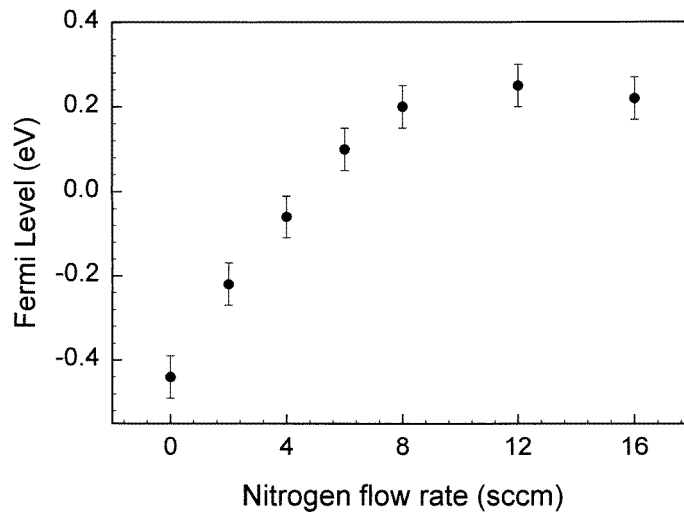


Figure 5. The Fermi level with respect to nitrogen flow rate.

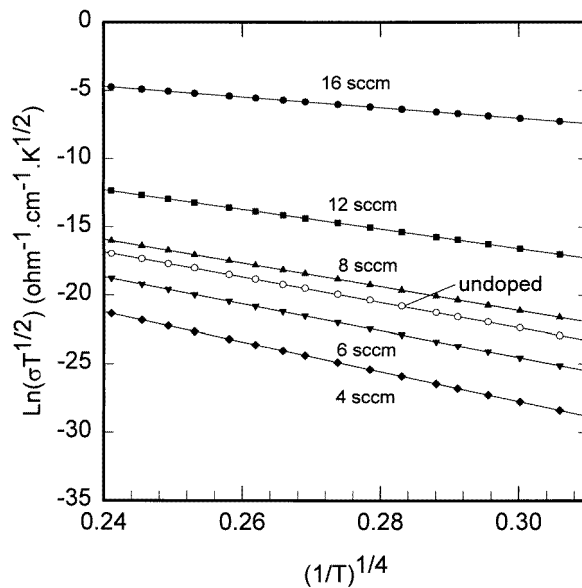


Figure 6. The relations between $\ln(\sigma T^{1/2})$ and $T^{-1/4}$ in the temperature range from 100 to 300 K for as-deposited and N-doped ta-C films.

As the Arrhenius plots of the conductivity deviate from a straight line at the temperature below 300 K (figure 2), the temperature dependences of the conductivity of as-deposited and N-doped ta-C films are shown in figure 6 as $\ln(\sigma T^{1/2})$ versus $T^{-1/4}$. It can be seen that a linear relationship exists between $\ln(\sigma T^{1/2})$ and $T^{-1/4}$ for all the films. This indicates that the dominant electronic transport mechanism in the low temperature range is the variable range hopping by a tunnelling process near the Fermi level. From the variable range hopping transport, valuable information on the density of states at the Fermi level can be extracted.

Although the $T^{-1/4}$ dependence of $\ln(\sigma T^{1/2})$ was widely observed by Veerasamy [13] in nitrogen-doped ta-C, by Fontaine *et al* in boron implanted a-C [21] and by Praver *et al* in diamond-like carbon thin films [22], details of the density of states at the Fermi level were not taken into account in their papers. Because of the absence of an appropriate band model for amorphous carbon, the Mott model [23] was used to deal with the conductivity in the low temperature range. From the Mott model, we can obtain the following expressions [24],

$$N(E_F) = 24\pi^2 \frac{k^2 S^2}{e^6 v_{ph}^3} \exp^3(x_0) \quad (1)$$

$$\alpha = \frac{3\pi}{4} \frac{kS^2}{e^2 v_{ph}} \exp(x_0) \quad (2)$$

$$R = \left[\frac{9}{8\pi\alpha N(E_F)kT} \right]^{1/4} \quad (3)$$

where $N(E_F)$ is the density of states at the Fermi level, α is a quantity which is representative for the rate of localization of the wave function at a site, R is the most probable hopping distance, k the Boltzmann constant, e the electronic charge, v_{ph} the phonon attempt frequency, assumed to be 10^{14} s^{-1} [25], S is the slope of the plot $\ln[\sigma(T)T^{1/2}]$ against $T^{-1/4}$ and x_0 is the intercept at $T^{-1/4} = 0$. The density of states $N(E_F)$ around the Fermi level, the hopping characteristic temperature T_0 [24], the rate of the localized electron wave function α and the hopping distance at 100 K deduced from figure 6 are given in table 1.

Table 1. VRH characteristic temperature T_0 , density of states $N(E_F)$ at the Fermi level, radius of the localized electron wave function α^{-1} and most probable hopping distance at 100 K deduced from Mott's law for as-deposited and nitrogen-doped ta-C films.

Nitrogen flow rate (sccm)	T_0 (K)	$N(E_F)$ ($\text{cm}^{-3} \text{ eV}^{-1}$)	α^{-1} (\AA)	R (\AA)
0	7.27×10^7	3.3×10^{19}	4.5	49
4	1.39×10^8	9.7×10^{18}	5.4	69
6	9.17×10^7	7.9×10^{18}	6.6	77
8	5.62×10^7	7.1×10^{18}	8.1	83
12	2.63×10^7	5.4×10^{18}	11	97
16	2.26×10^6	6.5×10^{17}	52	241

From table 1, we can see that the largest VRH characteristic temperature, $1.39 \times 10^8 \text{ K}$ for 4 sccm N-doped film, is in the same range as that of a-Si:H ($\sim 10^8 \text{ K}$). The density of states near the Fermi level monotonically decreases from $3.3 \times 10^{19} \text{ cm}^{-3} \text{ eV}^{-1}$ for as-deposited ta-C film to $6.5 \times 10^{17} \text{ cm}^{-3} \text{ eV}^{-1}$ for 16 sccm N-doped film. The nearly two orders of magnitude decrease in the density of states near the Fermi level is due to the auto-compensation explained before. This indicates that nitrogen is a good dopant to modify the band structure of ta-C film. The radius of the localized electron wave function α^{-1} for as-deposited ta-C film (4.5 \AA) is about three times the shortest C-C distance and is in good agreement with the reduced RDF measurement [26]. As the nitrogen flow rate increases from null to 16 sccm, the radius of the localized electron wave function increases from 4.5 to 52 \AA , and the hopping distance at 100 K increases from 49 to 241 \AA . The increase in the radius of the localized electron wave function and the most probable hopping distance also result in the increase of the conductivity. In equation (1) and (2), k and e are

constant, S and x_0 can be obtained from the $\ln(\sigma T^{1/2})$ versus $T^{-1/4}$ plot, so the phonon attempt frequency ν_{ph} plays an important role in calculating the density of states near the Fermi level and the radius of the localized electron wave function. In our calculation, we used the data of hydrogenated amorphous carbon given by Robertson [25]. The accurate value of ν_{ph} for as-deposited and nitrogen-doped ta-C films needs further research.

4. Discussion

The electronic transport process in amorphous semiconductor can be divided into three conduction mechanisms, namely the conduction in extended states, the conduction in band tails and the conduction in localized states at Fermi level. When temperature is high enough, the carriers can be thermally activated to the extended states and the electronic transport process is the same as that in a crystal semiconductor. For the localized states at band tails or near the Fermi level, the conductance can only occur via a phonon-assisted thermally activated hopping or tunnelling process, and the conductance between two localized sites exponentially depends on both the spatial distance of the sites and the site energies (all energies are given with respect to Fermi level). When the thermal activation energy is enough to overcome the energy barrier among the localized states, the electron (hole) can hop to the nearest neighbours. This behaviour corresponds to the transport in band tails or is called 'nearest neighbours' hopping (NNH). The effective correlation energy, U , is negative for a threefold sp^2 site in the amorphous carbon network when it pairs up with another sp^2 site to form a π bond. So the sp^2 sites have a tendency to clustering separate π bonding sp^2 rings into a sizable graphite cluster. Based on Robertson's 'cluster model' for an amorphous carbon network [27], we can treat the C amorphous network as a few sp^2 clusters embedded in a sp^3 bonded matrix. While the sp^3 matrix controls the mechanical properties, the π states of the sp^2 cluster control the films' electronic structure and optical band gap, which depends on the mean cluster size. The gap of the σ states is about 5.5 eV which is much wider than that of π states, so the sp^3 bonded matrix forms a NNH tunnelling barrier between the cluster. For ta-C films deposited by the FCVA technique, the sp^3 content can reach 87% and the sp^2 sites can only form small clusters, or even π -bonded pairs. The observed 2.7 eV optical band gap for the films deposited under the condition of nitrogen flow rate less than 4 sccm is then probably due to the non-aligned π bonds. The smaller sp^2 cluster size implies a reduced width of the sp^3 matrix and makes a less effective tunnel barrier [28]. This is consistent with the fact that the activation energy for the thermal activated hopping to the band tails is much lower for our ta-C films (0.1–0.2 eV) than that of the a-C:H (0.3–0.4 eV) deposited by the CVD method which has a lower sp^3 fraction. When the temperature is low enough that the energy barrier to the nearest neighbour is larger than the thermal activated energy the NNH cannot happen because the sp^2 cluster is in a potential well of the sp^3 matrix. The conductance can only occur via a tunnelling process between two sp^3 sites at the Fermi level where the site energy and the site energy difference are both zero and produce a maximum equilibrium hopping rate. The hopping conduction takes place between localized levels from sp^3 carbon dangling bonds.

The variation of the electrical conductivity as well as the Fermi level shift with the change in doping concentration is an obvious evidence of a doping effect. The substitution doping of N remains weak even though N flow rate is high. This is evidenced by the relatively high activation energy (~ 0.6 eV) at N flow rate of 16 sccm. The various possible C–N bonding configurations were proposed by Robertson and Davis [8] for N in the C amorphous network. Because of the coordination environment in the disordered material, the atom can self-adjust to satisfy the $8 - N$ rule requirement at the atom site, and only a

small portion of N atoms can form the doping configuration $N_{4\sigma}$ and $N_{3\sigma}$ bonding. This also gives an explanation for the very low efficiency of the N doping. In the lightly doped regime (nitrogen flow rate less than 4 sccm), the C amorphous network remain a highly tetrahedral structure and the incorporated N atoms are substantially in the sp^3 site. This can be verified by the fact that the optical band gap, which is dominated by the sp^2 cluster size, keeps constant in this region and is consistent with the electron diffraction study results by Davis *et al* [26]. At a low N concentration, the predominantly tetrahedral structure of ta-C is unaffected by the incorporation of the N atoms, though there is an increase in bond angle from 109.6° to 113° deduced from the radial distribution function (RDF) [26]. In the highly doped regime, the predominant C–N bonding is a trigonal bond (non-doping pyridine-like bonding, non-doping pyrrole-like bonding and doping $N_{3\pi}$ bonding). This can be interpreted as the increasing N sites in the C amorphous network reducing the energy barrier for sp^3 to sp^2 transition to a small value, so that the graphitization proceeds around the N site. This results in a broadening of the π and π^* bands and a narrow optical band gap.

5. Conclusion

Nitrogen is an n-type dopant of the tetrahedral amorphous carbon thin films. With the increasing N flow rate from null to 16 sccm (nitrogen partial pressure from 0 to 2.4×10^{-4} Torr), the Fermi level shifts from 0.91 eV above the valence band to 0.65 eV below the conduction band. At the same time, the optical band gap measured by the spectral ellipsometer drops from 2.7 eV to 1.8 eV. Three electronic transport mechanisms, namely, transport in extended states, in band tails by hopping and variable range hopping near the Fermi level, predominantly contribute to the conductivity successively in the temperature ranges from 450 to 380 K, from 380 K to room temperature and from room temperature to 100 K, respectively. The density of states near the Fermi level extracted from the variable range hopping parameters is in the range of $6.5 \times 10^{17} \text{ m}^{-3} \text{ eV}^{-1}$ – $3.3 \times 10^{19} \text{ cm}^{-3} \text{ eV}^{-1}$. The dominant doping configuration is substitution in the sp^3 coordination at low N concentration and adoption of sp^2 bonding at high N concentration.

Acknowledgments

The authors wish to acknowledge the help of Dr C Jeynes and Dr R Silva of Surrey University, UK, for carrying out the Rutherford back-scattering measurements of the films.

References

- [1] Field J E (ed) 1979 *Properties of Diamond* (New York: Academic)
- [2] Shenai K, Scott R S and Baliga B J 1989 *IEEE Trans. Electron Devices* **36** 1811
- [3] Chan K K, Silva S R P and Amaratunga G A J 1992 *Thin Solid Films* **212** 232
- [4] Shi Xu, Tay B K, Tan H S, Li Z, Tu Y Q, Silva S R P and Milne W I 1996 *J. Appl. Phys.* **79** 7239
- [5] McKenzie D R, Mullar D and Pailthorpe B A 1991 *Phys. Rev. Lett.* **67** 773
- [6] Fallon P J, Verasamy V S, Davis C A, Robertson J, Amaratunga G A J, Milne W I and Koskinen J 1993 *Phys. Rev. B* **48** 4777
- [7] Robertson J 1992 *Surf. Coatings Technol.* **50** 185
- [8] Robertson J and Davis C A 1995 *Diamond Relat. Mater.* **4** 441
- [9] Shi X, Tu Y Q, Tan H S, Tay B K and Milne W I 1996 *IEEE Trans. Plasma Sci.* **24** 1309
- [10] Shi Xu, Flynn D, Tay B K, Prawer S, Nugent K W, Silva S R P, Lifshitz Y and Milne W I 1997 *Phil. Mag. B* **76** 351
- [11] Amaratunga G A J, Veerasamy V S, Davis C A, Milne W I, McKenzie D R, Yuan J and Weiler M 1993 *J. Non-Cryst. Solids* **164–166** 1119

- [12] Davis C A, McKenzie D R and Yin Y 1994 *Phil. Mag.* B **69** 1133
- [13] Veerasamy V S 1994 *PhD Thesis* Engineering Department, Cambridge University, UK
- [14] Shi Xu, Cheah L K and Tay B K 1998 *Thin Solid Films* **312** 166
- [15] Silva S R P, Robertson J, Amaratunga G A J, Rafferty B, Brown M, Schwan J, Franceschini D F and Maritto G 1997 *J. Appl. Phys.* **81** 2626
- [16] Veerasamy V S, Amaratunga G A J, Davis C A, Timbs A E, Milne W I and McKenzie D R 1993 *J. Phys.: Condens. Matter* **5** L169
- [17] Mott N F 1970 *Phil. Mag.* **22** 7
- [18] Frauenheim T, Stephan U, Blaudeck P and Jungnickel G 1994 *Diamond Relat. Mater.* **3** 462
- [19] Amaratunga G A J, Segal D E and Mckenzie D R 1991 *Appl. Phys. Lett.* **59** 69
- [20] Robertson J 1991 *Diamond and Diamond-Like Films and Coatings* ed R E Clausing et al (New York: Plenum) p 37
- [21] Fontaine F, Gheeraert E and Deneuille A 1996 *Diamond Relat. Mater.* **5** 752
- [22] Praver S, Ran B, Kalish R, Johnston C, Chalker P, Bull S J, McCabe A and Jones A M 1996 *Diamond Relat. Mater.* **5** 405
- [23] Mott N F 1969 *Phil. Mag.* **19** 835
- [24] Nagels P 1979 *Amorphous Semiconductors* ed M H Brodsky (Berlin: Springer)
- [25] Robertson J 1996 *J. Non-Cryst. Solids* **198–200** 615
- [26] Davis C A, Yin Y, McKenzie D R, Hall L, Kravtchinskaia E, Keast V, Amaratunga G A J and Verasamy V S 1994 *J. Non-Cryst. Solids* **170** 46
- [27] Robertson J 1995 *Diamond Relat. Mater.* **4** 297
- [28] Robertson J 1992 *Phil. Mag.* B **66** 199